

Intrinsic charm and the $D^+ - D^-$ asymmetry produced in proton-proton collisions

G.I. Lykasov¹, M.N. Sorokovikov¹, S.J. Brodsky²

January 27, 2025

¹*Joint Institute for Nuclear Research, 141980, Dubna, Moscow region, Russia*

²*SLAC National Accelerator Laboratory, Stanford University, Menlo Park, CA 94025, United States*

Abstract

We investigate the contribution of the charm-anticharm ($c\bar{c}$) asymmetry of the proton eigenstate obtained from QCD lattice gauge to the asymmetry of D^+ , D^- and D^0 , \bar{D}^0 mesons produced in pp collisions at large Feynman variables x . It is shown that an important tool for establishing the intrinsic charm (IC) content of the proton is the charm hadron-antihadron asymmetry formed in pp collisions. Predictions for the asymmetry as function of x for different IC probabilities are presented. We show that the interference of the intrinsic $|uudc\bar{c}\rangle$ Fock state with the standard contribution from the PQCD evolution leads to a large D^+D^- asymmetry at large Feynman x .

1. Introduction

According to Quantum Chromodynamics (QCD), the heavy quarks in the nucleon sea have both perturbative *extrinsic* and non-perturbative intrinsic heavy quark (IQ) components. The extrinsic sea quarks arise from gluon splitting, which is triggered by a probe in the reaction. It can be calculated in QCD within perturbation theory. In contrast, the intrinsic sea quarks are contributions within the non-perturbative wave functions of the nucleon eigenstate which do not depend on the probe. The existence of non-perturbative intrinsic charm IC was originally proposed in the BHPS model [1] and developed further in subsequent papers [2–4].

In Light-Front (LF) Hamiltonian theory, the intrinsic heavy quarks of the proton are associated with non-valence Fock states, such as the $|uudQ\bar{Q}\rangle$ Fock state in the hadronic proton eigenstate of the LF Hamiltonian; this implies that the heavy quarks are multi-connected to the valence quarks, and thus have a probability which scales as $\frac{1}{M_Q^2}$ or faster. Since the LF wave function is maximal at minimum off-shell invariant mass; i.e., at equal rapidity, the intrinsic heavy quarks carry large light-front momentum fraction x_Q in the hadronic eigenstate.

The concept of intrinsic heavy quarks has also been proposed in the context of meson-baryon fluctuations [6, 7], where intrinsic charm is identified with the two-body hadron state $\bar{D}^0(u\bar{c})\Lambda_c^+(udc)$ in the proton. Since these heavy quark distributions depend on the nonperturbative correlations within the hadronic LF eigenfunction, they also represent *intrinsic* contributions to the hadron's fundamental structure.

A key characteristic of the non-valence LF wave functions is the distinctly different momentum and spin distributions for the intrinsic Q and anti-quark \bar{Q} in the nucleon; for example, in the case of the charm-anticharm asymmetry, the comoving heavy sea quarks are sensitive to the global quantum numbers of the nucleon [5]. Furthermore, since all of the intrinsic quarks in the $|uudQ\bar{Q}\rangle$ Fock state have similar rapidities, they can re-interact, again, leading to significant Q vs \bar{Q} asymmetries; i.e., large asymmetries in the charm versus charm momentum and spin distributions. The heavy quark asymmetry can also arise from the interference of the amplitudes corresponding to the intrinsic and extrinsic contributions.

Recently a new prediction for the non-perturbative intrinsic charm-anticharm asymmetry of the proton eigenstate has been obtained from a QCD lattice gauge theory calculation of the proton's $G_E^p(Q^2)$ form factor [9]. This form factor arises from the fact that the non-valence quarks and anti-quarks have different distributions in the proton's eigenstate. This result, together with the exclusive-inclusive connection and analytic constraints on the form of hadronic structure functions from Light-Front Holographic QCD (LFHQCD) [10], predicts a significant non-perturbative $c(x, Q) - \bar{c}(x, Q)$ asymmetry in the proton structure function at high x , consistent with the dynamical features predicted by intrinsic charm models.

A recent measurement of the $c\bar{c}$ asymmetry has been reported by the NNPDF collaboration [11]. The nonzero asymmetry between the D and \bar{D} mesons extracted from $Z + c$ production observed by the LHCb experiment in pp collision [15] and at EIC experiment [16] in eA collisions can be attributed to the IC contribution in the nucleon PDF. There are also interesting papers on the IC contribution to the proton PDF [17–19] and [20].

Despite intensive studies, the hypothesis of the non-zero intrinsic heavy quark contribution in the proton PDF [1] has not yet been definitively confirmed by experiment. There have been many attempts to confirm or estimate the IQ probability in the proton from experimental data; see [12] and references therein. For example, the latest global analysis [13] shows that there is local evidence of the IC in the interval $0.3 < x < 0.6$ with confidence level CL of order 3σ . According to this analysis, the average fraction of the intrinsic charm quark is about $\langle x_c \rangle = 0.62 \pm 0.28\%$, including the PDF uncertainties. However, the inclusion of missing high order uncertainties (MHOU) results in $\langle x_c \rangle = 0.62 \pm 0.61\%$, which is due to the large contribution of MHOU at $x < 0.2$. The reason for the large MHOU is related to the inclusion both 4FNS (four flavor number scheme), NNLO charm PDF determined from data, and 3FNS (three flavor number scheme, intrinsic) charm PDF within NNNLO corrections. Thus the determination of the IC content in the proton by analyzing only inclusive spectra of heavy hadrons or c -jets produced in pp collisions at LHC energies has proved to be very complicated. Apart from these uncertainties, there are statistical and systematical errors [14]. In other words, various corrections to the LO approximation of the inclusive spectra calculations can reduce the evidence for IC contribution. However, as we emphasize here, the heavy hadron production asymmetries, for example, $D^+ D^-$ mesons produced in pp collisions, are sensitive to the IC contribution since the nonperturbative $c\bar{c}$ pair is asymmetric.

In this paper we analyze the heavy hadron asymmetry arising from nonperturbative sources of intrinsic charm in detail. For the calculation of the inclusive D -meson spectra and the $D \bar{D}$ asymmetry in pp collisions, we use the quark-gluon string model (QGSM). A short review of this approach and the scheme-dependence of its predictions is presented in Sect.2. We then show why the asymmetry of $D \bar{D}$ mesons can be an ideal tool for identifying the IC content in the proton in comparison to the inclusive D -meson inclusive spectra.

2. Charmed hadron production in pp collisions within QGSM without IC

The quark-gluon string model (QGSM) is based on the $1/N$ topological expansion of the amplitude of hadron-hadron interaction in the s -channel, which is related to its t -channel expansion over Regge poles; here N is the number of flavors or colors [21–24]. This theory allows one to describe the data on hadron production in pp collisions at high energies and large x rather satisfactorily ([25]– [33]). The charmed hadron production in pp collisions was considered recently within the QGSM in [29], where it was applied to the analysis of the atmospheric neutrino flux. The satisfactory description of NA27 data [31] for both charmed mesons and charmed baryons produced in pp collisions at the initial proton energy ~ 400 GeV was demonstrated. In ref. [29] the IC content in the proton was not included because the NA27 data were measured at $x \leq 0.4$, where the IC contribution plays a minor role. We will apply the QGSM to estimate the asymmetry of D, \bar{D} mesons produced in pp collisions, including the IC content in the proton.

The inclusive spectrum of hadrons produced in pp collisions as a function of the Feynman variable x within the QGSM is presented in the following form [28, 29]:

$$\rho_h(x) = \int E \frac{d^3\sigma}{d^3p} d^2p_\perp = \sum_{n=0}^{\infty} \sigma_n(s) \varphi_n^h(s, x), \quad (1)$$

where $\sigma_n(s)$ is the cross section of $2n$ -strings (chains) production, corresponding to the s -channel discontinuity of the multi-pomeron diagrams. The analysis is performed for pomerons with n cuts and an arbitrary number of external pomerons taking into account elastic re-scattering. Here $\varphi_n^h(s, x)$ is the x -distribution of the hadron h produced in the fission of $2n$ quark-gluon strings: $\varphi_0^h(s, x)$ accounts for the contribution of the diffraction dissociation of colliding hadrons, $n = 1$ corresponds to the strings formed by valence quarks and diquarks; terms with $n > 1$ are related to sea quarks and antiquarks.

The cross sections $\sigma_n(s)$ were calculated [26] in the quasi-eikonal approximation which accounts for the low-mass diffractive excitation of the colliding particles and corresponds to maximum inelastic diffraction consistent with the unitarity condition. Only non-exchanged graphs were considered, neglecting the interactions between pomerons.

In the case of D meson production in pp interaction, the functions $\varphi_n^h(s, x)$ can be written [27] as follows:

$$\varphi_n^D(s, x) = a^D \left\{ F_{qv}^{D(n)}(x_+) F_{qq}^{D(n)}(x_-) + F_{qq}^{D(n)}(x_+) F_{qv}^{D(n)}(x_-) \right. \quad (2)$$

$$\left. + 2(n-1) F_{q\text{sea}}^{D(n)}(x_+) F_{\bar{q}\text{sea}}^{D(n)}(x_-) \right\}, \quad (3)$$

where $x_\pm(s) = \frac{1}{2} \left[\sqrt{x^2 + 4m_\perp^2/s} \pm x \right]$.

The functions $F_{qv}^{D(n)}(x_\pm)$, $F_{qq}^{D(n)}(x_\pm)$, and $F_{q\text{sea}}^{D(n)}(x_\pm)$, $F_{\bar{q}\text{sea}}^{D(n)}(x_\pm)$ are defined as the convolution of the quark distributions with the fragmentation functions, taking into account contributions of the valence quarks, diquarks, and sea quarks, antiquarks. For example, in pp collisions [28, 30, 32]:

$$F_{qv}^{D(n)}(x_\pm) = \frac{2}{3} \int_{x_\pm}^1 f_p^{uv(n)}(x_1) G_u^D(x_\pm/x_1) dx_1 + \quad (4)$$

$$+ \frac{1}{3} \int_{x_\pm}^1 f_p^{dv(n)}(x_1) G_d^D(x_\pm/x_1) dx_1,$$

$$\begin{aligned}
F_{qq}^{D(n)}(x_{\pm}) &= \frac{2}{3} \int_{x_{\pm}}^1 f_p^{ud(n)}(x_1) G_{ud}^D(x_{\pm}/x_1) dx_1 + \\
&+ \frac{1}{3} \int_{x_{\pm}}^1 f_p^{uu(n)}(x_1) G_{uu}^D(x_{\pm}/x_1) dx_1.
\end{aligned} \tag{5}$$

There are similar forms for $F_{q_{\text{sea}}}^{D(n)}(x_+)$ and $F_{q_{\text{sea}}}^{D(n)}(x_-)$. At the limits $x \rightarrow 0$ and $x \rightarrow 1$, these functions are defined by Regge asymptotics. At intermediate values of x , an interpolation is used [27, 28, 30]. In particular,

$$f_p^{uv(n)}(x) = C_n^{uv} x^{-\alpha_R(0)} (1-x)^{\alpha_R(0)-2\alpha_N(0)+n-1}, \tag{6}$$

$$G_d^{D^-}(x/x_1) = G_{\bar{u}}^{D^0}(x/x_1) = (1-x/x_1)^{\lambda-\alpha_{\psi}(0)} [1 + a_1(x/x_1)^2], \tag{7}$$

and the ud diquark has the following x -dependence:

$$f_p^{ud(n)}(x) = C_n^{ud} (1-x)^{-\alpha_R(0)} x^{\alpha_R(0)-2\alpha_N(0)+n-1}, \tag{8}$$

where $\alpha_R(0) = 0.5$, $\alpha_N(0) = -0.5$, $\alpha_{\psi}(0) = -2.2$, $\lambda = 2 < p_{\perp}^2 > \alpha'_R = 0.5$.

The coefficient C_n^{uv} is determined by the normalization $\int_0^1 f_p^{uv(n)}(x) dx = 1$. One can see from Eqs. (6,8) that the diquark distribution increases as $(1-x)^{-\alpha_R(0)}$, and the valence quark distribution decreases as $(1-x)^{\alpha_R(0)-2\alpha_N(0)+n-1}$, when x grows. More details on the functions $\varphi_n^h(s, x)$, $f_p^j(x)$ and $G_j^D(x/x_1)$ can be found in ref. [27, 28, 30, 32, 33].

We note that the sea quark distributions within the QGSM have the same forms as the valence quarks; however, they contribute to inclusive hadron spectra starting from two-pomeron exchange, i. e., at $n \geq 2$.

The distribution of the sea charmed quark in the proton has the following form within the QGSM [32] (Appendix B):

$$f_{c\bar{c}}^{(n)} = C_{c\bar{c}} \delta_{c\bar{c}} x^{a_c} (1-x)^{b_c^n}, \tag{9}$$

where $a_c = -\alpha_{\psi}(0)$ and $b_c^n = 2\alpha_R(0) - 2\alpha_N(0) - \alpha_{\psi}(0) + n - 1$ are presented in [32], TABLE VII; $\delta_{c\bar{c}}$ is the weight of the sea $c\bar{c}$ in the proton. The coefficient $C_{c\bar{c}}$ is determined from the normalization condition

$$\int_0^1 f_{c\bar{c}}^{(n)}(x) dx = C_{c\bar{c}} \tag{10}$$

$$C_{c\bar{c}} = \frac{\Gamma(2 + a_c + b_c^n)}{\Gamma(1 + a_c) \Gamma(1 + b_c^n)}. \tag{11}$$

Here $\Gamma(\alpha)$ is the gamma function. The distribution of the sea bottom quark in proton has the following form within QGSM [32]:

$$f_{b(\bar{b})}^{(n)} = C_{b(\bar{b})} \delta_{b(\bar{b})} x_b^a (1-x)^{b_b^n}, \tag{12}$$

where $a_b = -\alpha_Y(0)$ and $b_b^n = 2\alpha_R(0) - 2\alpha_N(0) - \alpha_Y(0) + n - 1$, $\delta_{b(\bar{b})}$ is the weight of the sea $b\bar{b}$ pairs in the proton. The normalization coefficient $C_{b(\bar{b})}$ has the similar form as Eq. (11) by replacing a_c, b_c^n into a_b, b_b^n .

3. Charmed hadron production in pp collisions within the QGSM including IC

We now include the contribution of IC in the sea charmed quark distributions obtained within the QGSM. We modify Eq. (9) to the form

$$f_{c\bar{c}}^{(n)}(x) \rightarrow (1-w)f_{c\bar{c}}^{(n)}(x) + wf_{c\bar{c}}^{in}(x), \quad (13)$$

where w is the probability of the IC contribution in the proton and $f_{c\bar{c}}^{in}$ is the intrinsic charm contribution to the conventional charm distribution $f_{c\bar{c}}^{(n)}(x)$ at $n \geq 2$ given by Eq. (9). The form of $f_{c\bar{c}}^{in}$ in the case of a symmetric $c\bar{c}$ sea in the proton, calculated within the BHPS model [1, 34] at $Q^2 = m_c^2$, has the following form [35]:

$$f_{c\bar{c}}^{in}(x) = 600x^2 \{ (1-x)(x^2 + 10x + 1) + 6x(x+1)\ln(x) \}, \quad (14)$$

with the normalization condition

$$\int_0^1 f_{c\bar{c}}^{in}(x) dx = 1. \quad (15)$$

The asymmetric intrinsic $f_{c(\bar{c})}^{in}(x)$ distributions obtained within the meson cloud-model, where the $|uudc\bar{c}\rangle$ Fock state can be identified with the $|\Lambda_{udc}D_{u\bar{c}}\rangle$ off-shell excitation of the proton. This distribution is parameterized in the following form [37]:

$$f_c^{in}(x) = Bx^{1.897}(1-x)^{6.095} \quad (16)$$

and

$$f_{\bar{c}}^{in}(x) = \bar{B}x^{2.5}(1-x)^{4.929}, \quad (17)$$

where B/\bar{B} is determined by the quark number sum rule :

$$\int_0^1 \{ f_c^{in}(x) - f_{\bar{c}}^{in}(x) \} dx = 0. \quad (18)$$

Generally the probability of the intrinsic heavy quark-anti quark $Q\bar{Q}$ contribution in the proton is proportional to $1/M_Q^2$. It means that the coefficients B and \bar{B} are proportional to $1/M_Q^2$. The light-front x -distribution $f_{\bar{c}}^{in}(x)$ for the intrinsic \bar{c} quarks is calculated as follows:

$$f_{\bar{c}}^{in}(x) = f_c^{in}(x) - \Delta c(x), \quad (19)$$

where the difference $\Delta c(x) = [c(x) - \bar{c}(x)]$, obtained using lattice QCD, was taken from [9].

In Fig. (1) the inclusive x -spectrum of D^0 mesons produced in pp collisions at the initial energy in the laboratory system $E_{lab} = 400$ GeV ($\sqrt{s} = 27.42$ GeV) is presented. One can observe a good description of NA27 data for D^0 -mesons. The results are presented at different values of the IC probabilities $\omega = 0.01$ (BHPS1) and $\omega = 0.035$ (BHPS2), including both the important interference effect and without it; see Appendix. One can see that the maximum signal of the IC contribution to the spectrum is less than 1%. The NA27 data on D^\pm meson [31] production have large error bars, much larger than the data on $D^0(\bar{D}^0)$; therefore, we compare our calculations with the data for $D^0(\bar{D}^0)$ mesons.

An unfortunate effect of the asymmetric IC contribution is invisible in the x -spectrum presented in Fig.1. This is due to the fast decrease of the intrinsic c -quark distribution,

calculated within the meson cloud model, according to Eq. (16) [37], compared to the increasing diquark contribution at large x , as $1/(1-x)^{1/2}$, according to Eq. 8. It leads to the dominant contribution of the diquark distribution to the x -spectrum at large x . Therefore, the distributions of sea quarks give a negligibly small contributions at large x . However, in contrast to that, the effect of the asymmetric IC can be visible in the asymmetry of D^-, D^+ mesons produced in pp collisions, as it will be shown in the next section. The fragmentation functions of quarks and diquarks into D^0, \bar{D}^0 and D^-, D^+ mesons are presented in the Appendix.

4. Alternative approach for identifying the IC content in the proton within the QGSM

There is another approach for investigation of the IC content in the proton within the QGSM, which was suggested in ref. [40]. Intrinsic quarks are valence-like quarks, according to [1]. That is why in ref. [40], the intrinsic c -quark (anti quark) x -distributions in the proton, which are calculated within the QGSM, have the forms similar to those of valence quark distributions.

The sea $c(\bar{c})$ and $b(\bar{b})$ quark distributions within the QGSM [23, 24, 32] are presented in Eqs. (9,12). At low x the c -quark distribution is proportional to $x^{-\alpha_\psi(0)}$, whereas the valence quark distributions are proportional to $x^{-\alpha_R(0)}$; $\alpha_\psi(0)$ is the intercept of the ψ -trajectory, and $\alpha_R(0)$ is the intercept of the Reggeon trajectory. These intercepts are very different: $\alpha_\psi(0) = 0$ or -2.2 and $\alpha_R(0) = 1/2$. In [40] the sea $c(\bar{c})$ quark distribution in the proton is parameterized similarly to the valence quark distribution:

$$f_{c\bar{c}}(x, n) = C_c x^{-\alpha_R(0)} (1-x)^{n+1}; n > 1 \quad (20)$$

The sea quark distributions $f_{u(\bar{u})}, f_{d(\bar{d})}$ and $f_{s(\bar{s})}$ in [40] are parameterized in the following forms:

$$f_{u(\bar{u})}^{sea}(x, n) = f_{d(\bar{d})}^{sea}(x, n) = C_{\bar{u}} x^{-\alpha_R(0)} [(1 + \delta/2)(1-x)^{n+\alpha_R(0)}(1-x/3) - \delta/2(1-x)^{n+1}], n > 1 \quad (21)$$

$$f_s^{sea}(x, n) = C_s x^{-\alpha_R(0)} (1-x)^{n+1}, n > 1,$$

The convolutions of sea quarks with their fragmentation functions to the D -meson, see Eqs. (5,6), are given in the following forms:

$$F_{q_{sea}}^{D(n)}(x_\pm) = \frac{1}{2 + \delta_s + \delta_c} [F_{u_{sea}}^{D(n)} + F_{d_{sea}}^{D(n)} + \delta_s F_{s_{sea}}^{D(n)} + \delta_c F_{q_{sea}}^{D(n)}] \quad (22)$$

The fragmentation functions (FF) of c, \bar{c} quarks to D mesons were taken from [40] in the forms similar to the FF into K -mesons, namely:

$$G_{(c+\bar{c})/2}^{D^+} = G_{(c+\bar{c})/2}^{D^0} = G_{(c+\bar{c})/2}^{\bar{D}^0} = G_{(c+\bar{c})/2}^{D^-} = [a_{c0} z(1-z)^{\lambda-\alpha_R(0)} + a_{c1} (1-z)^{1+\lambda-\alpha_R(0)}], \quad (23)$$

where $a_{c0} = 0.68$, $a_{c1} = 0.26$; $\alpha_R(0) = 1/2$; $\delta = \delta_s + \delta_c$. Here $\delta_s = 0.2$ and $\delta_c = 0.04$ are the relative probabilities of strange and charmed quarks existing in the proton sea [40].

In order to compare our calculations within the QGSM with the similar calculations done in [40], we present the following ratios R_1, \dots, R_4 :

$$R_1 = ((\frac{d\sigma}{dx})_1 \text{ at } \delta_c = 0.01, \delta_s = 0.2) / \sigma_s$$

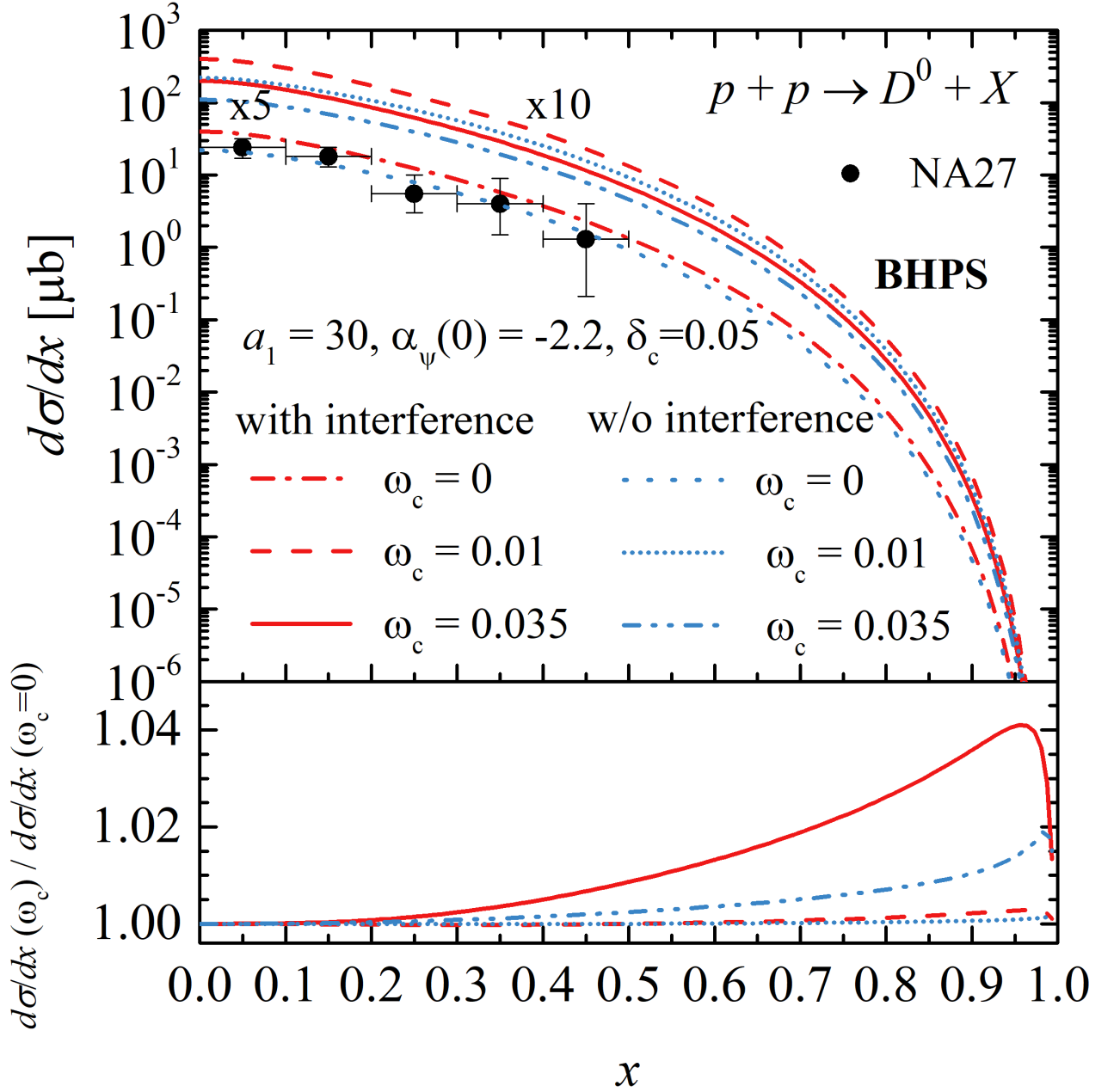


Figure 1: The x -distribution of the inclusive spectrum of D^0 -mesons produced in pp collisions at the initial energy $E_{lab} = 400$ GeV and $0 \leq x \leq 1$. Top: the inclusive spectrum at different values of ω with and without (w/o) the interference of the quark (diquark) and the sea quark (extrinsic and intrinsic) amplitudes. The interference between the extrinsic and intrinsic quark contributions are also taken into account; see Appendix. The NA27 data were taken from [31]. Bottom: the ratio of the x -spectrum for the nonzero IC probability ω_c to the spectrum at $\omega_c = 0$, with interference and without it. With interference: solid red line at $\omega_c = 0.035$, dashed red line at $\omega_c = 0.01$. Without interference (w/o): double dashed blue line at $\omega_c = 0.035$, dotted blue line at $\omega_c = 0.01$. The calculations were done using the IC distributions in forms of Eqs.(16,17), labeled as **BHPS**.

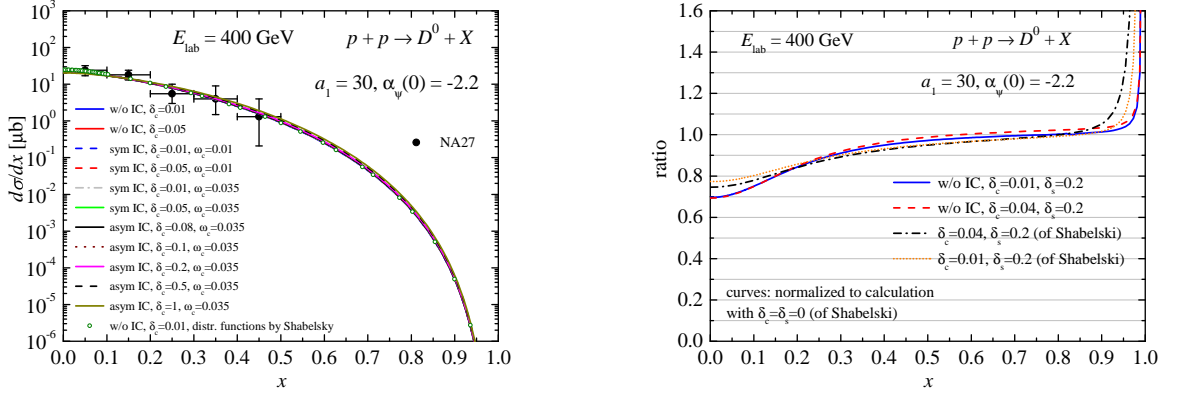


Figure 2: Left: our calculation of the inclusive x -spectrum of D^0 -mesons produced in pp collisions at the initial energy $E_{lab} = 400$ GeV with different values of the weight δ_c and the IC probability w_c . The open circles correspond to the calculation of ref. [40]. Right: the blue solid line is the ratio R_1 , the red dashed line is R_2 , the black dash-dotted line is R_3 and the orange dotted line is R_4 .

$$R_2 = \left(\left(\frac{d\sigma}{dx} \right)_2 \text{ at } \delta_c = 0.04, \delta_s = 0.2 \right) / \sigma_s$$

$$R_3 = \left(\left(\frac{d\sigma}{dx} \right)_S \text{ at } \delta_c = 0.04, \delta_s = 0.2 \right) / \sigma_s$$

$$R_4 = \left(\left(\frac{d\sigma}{dx} \right)_S \text{ at } \delta_c = 0.01, \delta_s = 0.2 \right) / \sigma_s,$$

where $\sigma_s \equiv \frac{d\sigma}{dx}$ is calculated within the QGSM in ref. [40] using sea quark distributions at $\delta_c = 0, \delta_s = 0$; $\left(\frac{d\sigma}{dx} \right)_{1,2}$ is the x -spectrum of $D^0(\bar{D}^0)$ calculated within the QGSM in this paper; $\left(\frac{d\sigma}{dx} \right)_S$ is the x -spectrum calculated in [40]. In Fig. (2, left), the x -spectrum of D^0 -mesons produced in pp collisions at $\sqrt{s} = 27$ GeV is presented for different weights of the sea $c\bar{c}$ and $s\bar{s}$ pairs and the IC weight w_c . One can see from this panel, that its sensitivity to these parameters is very small. In Fig. (2, right) the ratios R_1, \dots, R_4 are presented as functions of x . The difference between our calculation within the QGSM from the one within the model of [40] is about 10%-13% at small $0 \leq x \leq 0.15$. This is due to different forms of the sea quark distribution. In [40] it is assumed that both the extrinsic and intrinsic charm quarks have the same distributions as the valence quarks $f_p^{u_v^n}(x), f_p^{d_v^n}(x)$ at $n > 1$, where n is the number of exchanged Pomerons or $2n$ quark-antiquark pairs. In some sense, the charmed and strange quarks have valence-like distributions, as it was assumed for the intrinsic $Q\bar{Q}$ pairs in [1]. In [40] the weight δ_c of sea $c\bar{c}$ pairs includes both extrinsic and intrinsic charmed quarks. Comparing Fig. (1) with Fig. (2), the question arises why there is no visible difference between the two QGSM approaches presented in Sections (2,3) and 4, although the c -quark distributions in proton are different. This is due to the main contribution of the diquark x -distribution at $x \rightarrow 1$, according to Eq.(8), compared to the valence quark distributions; see Eq.(6) at large x . Therefore, the inclusive x -spectra of D, \bar{D} -mesons are almost insensitive to the sea-quark distributions in the proton at large x . However, the asymmetry of D^+, D^- -mesons, as a function of x , can be visible at large x , as will be shown in the next section.

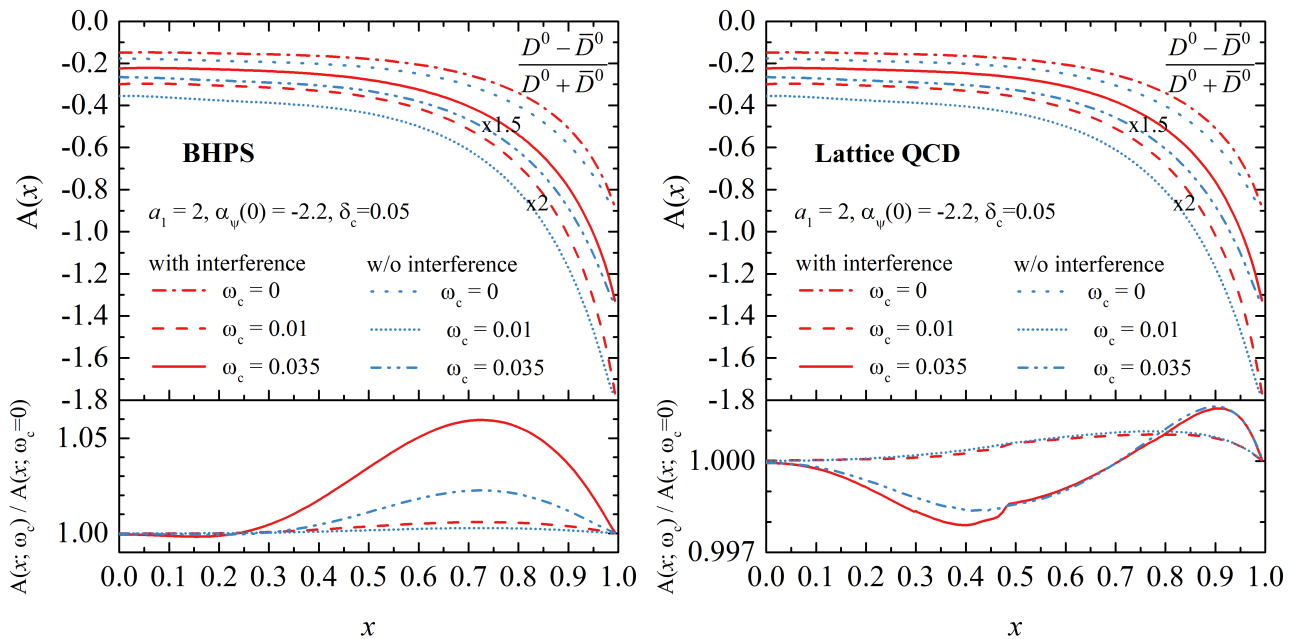


Figure 3: Left: the *Set 1* of x -distribution of asymmetry $A_{D^0\bar{D}^0}(x)$ between D^0 and \bar{D}^0 - mesons produced in pp collision at the initial energy $E_{lab} = 400$ GeV and $a_1 = 2$, and the ratio of the asymmetry with the non zero IC probability ω_c to the one with $\omega_c = 0$. The calculations were done using the IC distributions in forms of Eqs.(16,17). Right: the *Set 2* of asymmetry $A_{D^0\bar{D}^0}(x)$ using Eq.(16) for $f_c^{in}(x)$ and Eq.(17) for $f_{\bar{c}}^{in}(x)$. With interference: solid red line at $\omega_c = 0.035$, dashed red line at $\omega_c = 0.01$. Without interference (w/o): double dashed blue line at $\omega_c = 0.035$, dotted blue line at $\omega_c = 0.01$.

5. $D^0\bar{D}^0$ and D^-D^+ asymmetries in pp collisions

In an important recent development [9], the difference of the nonperturbative charm and anticharm quark distributions in the proton $\Delta c(x) = c(x) - \bar{c}(x)$ has been computed using lattice gauge theory. The predicted $\Delta c(x)$ distribution is non-zero at large $x \geq 0.4$, remarkably consistent with the expectations of intrinsic charm. The $c(x)$ vs. $\bar{c}(x)$ asymmetry can be understood physically by identifying the $|uudc\bar{c}\rangle$ Fock state with the $|\Lambda_{udc}D_{u\bar{c}}\rangle$ off-shell excitation of the proton.

Let us calculate the asymmetry $A_{D^0\bar{D}^0}(x)$ and $A_{D^-D^+}(x)$ for D -mesons produced in pp collisions, including the asymmetry between the intrinsic c -quark and \bar{c} quark as a function of x .

$$A_{D^0\bar{D}^0}(x) = \frac{d\sigma_{D^0}/dx - d\sigma_{\bar{D}^0}/dx}{d\sigma_{D^0}/dx + d\sigma_{\bar{D}^0}/dx} \quad (24)$$

$$A_{D^-D^+}(x) = \frac{d\sigma_{D^-}/dx - d\sigma_{D^+}/dx}{d\sigma_{D^-}/dx + d\sigma_{D^+}/dx} \quad (25)$$

The calculation of these asymmetries was done within two sets. The first one *Set 1* corresponds to use Eqs.(16,17) for distributions $f_c^{in}(x)$ and $f_{\bar{c}}^{in}(x)$ respectively obtained in [37] within the the meson cloudy bag model. *Set 2* was performed using Eq.16 for $f_c^{in}(x)$ and calculating $f_{\bar{c}}^{in}(x)$ from Eq. (19) because only $\Delta c(x)$ was calculated in [9] within the lattice QCD.

The results of $A_{D^0\bar{D}^0}(x)$ with different IC probabilities ω_c calculated within the QGSM are presented in Fig. 3. In the left panel the *Set 1* calculation is presented, whereas the

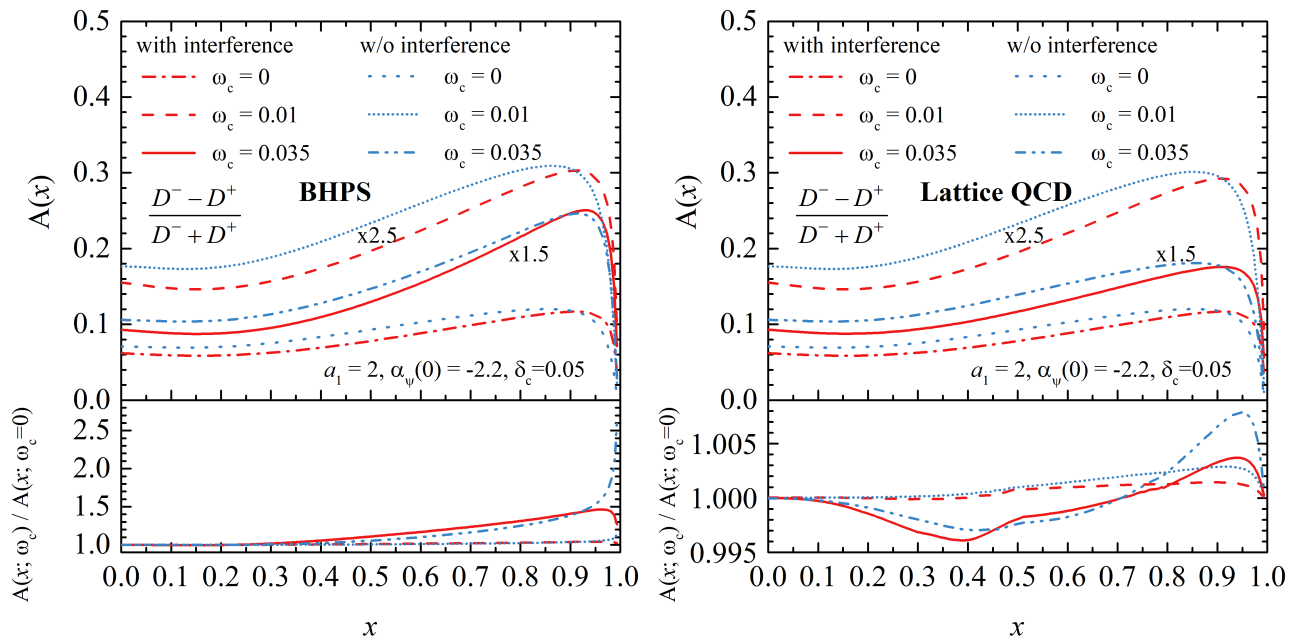


Figure 4: The plots for asymmetry $A_{D^-D^+}(x)$ with the same notations as in Fig.3.

Set 2 results are shown on the right. The calculations were done taking into account the interference between different parton contributions, also including the important interference between the contributions of extrinsic and intrinsic quarks; see Eqs.(26,27,28,29) in the Appendix.

The inclusion of the interference effects increases the asymmetry at $0 < x < 0.4$ by a maximum of (25-30)% for both calculations *Set 1* and *Set 2*, as it is seen in Fig. 3 (top). Both calculations show too small *IC* contribution for the $D^0\bar{D}^0$ asymmetry as it is seen from the bottom of this figure.

The asymmetry $A_{D^-D^+}(x)$ as a function of x using *Set 1* (left) and *Set 2* (right) is presented in Fig. 4. In the bottom of these plots, the ratios of the asymmetry for non-zero *IC* probability ω_c to the asymmetry at $\omega_c = 0$ are presented. The *Set 1* is more sensitive to the *IC* probability ω_c compared to *Set 2*, if we compare the bottom plots in Fig. 3. The difference between the left and right panels of Figs. (3,4) is due to the absence of information on the separate distributions $c(x)$ and $\bar{c}(x)$ obtained within the **Lattice QCD**, in [9] only $\Delta c(x)$ is presented. It is not sufficient to calculate the asymmetry precisely. The maximum value of the D^-D^+ asymmetry could be about 50% at $x \simeq 0.9$ at $a_1 = 2$ (right bottom in figure). Both bottom panels of Fig. 4 show a sizable sensitivity of the asymmetry to the interference effects at large x . The interference effects for the D^-D^+ asymmetry increase, when x grows, as Fig. 4 shows. Note that the interference between different amplitudes estimated in Appendix is maximal, when the relative phase angle between different amplitudes is approximately zero, i.e., the constructive sum of the amplitudes is calculated. The form of the $A_{D^-D^+}(x)$ enhancement at large x corresponding to the positive difference $d\sigma_{D^-}/dx - d\sigma_{D^+}/dx$ at $0.5 < x < 1.0$ is determined mainly by the FF of quarks and diquarks to D^- or D^+ , which describe the inclusive x -spectra of the open charm within the QGSM rather satisfactorily [23]- [33]. The FF used in our calculations of x -spectra and the asymmetries of D, \bar{D} -mesons are presented in the Appendix.

We note, that for the calculation of the asymmetries presented in Figs. (3,4) within the QGSM we used the charm (anti-charm) quark x -distributions $c(x)$ and $\bar{c}(x)$; therefore $\Delta c(x) = c(x) - \bar{c}(x)$ and asymmetries $A_{D^0\bar{D}^0}(x)$, $A_{D^-\bar{D}^+}(x)$ are shifted towards larger x in comparison to $x\Delta c(x)$, calculated within the lattice QCD in [9], and in the NNPDF

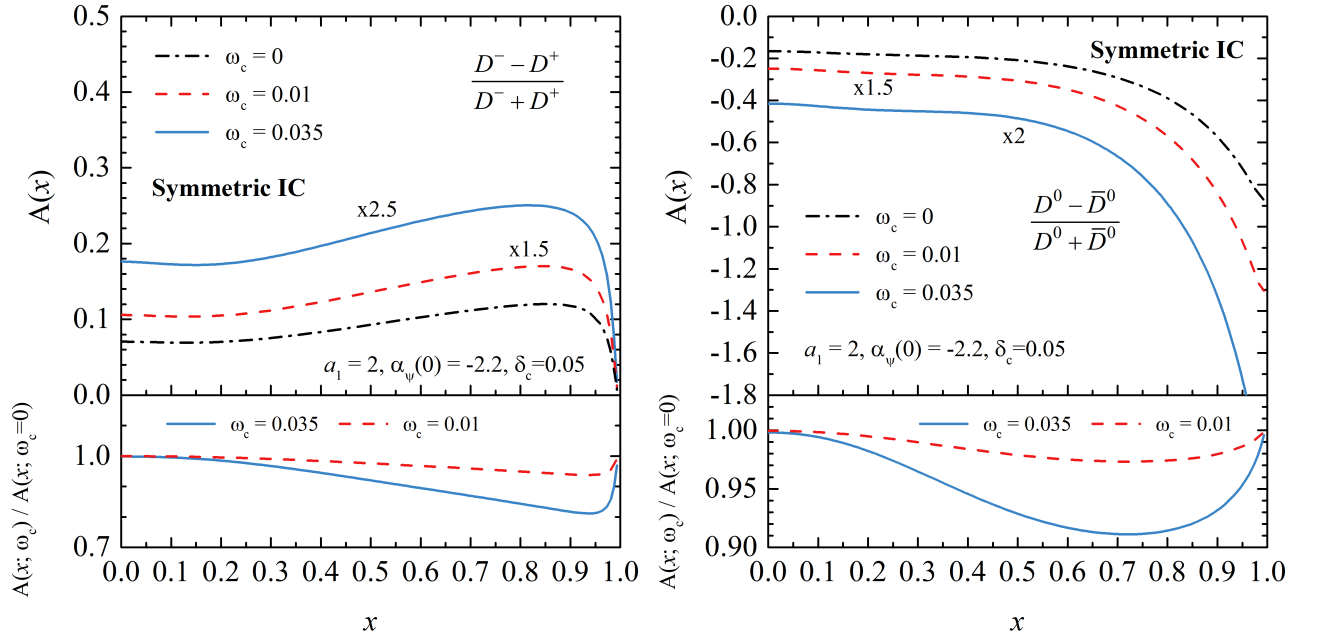


Figure 5: The plots of the asymmetries $A_{D^-D^+}(x)$ (left) and $A_{D^0\bar{D}^0}(x)$ (right) using the symmetric *IC* distribution, according to Eq. (13) with the same notations as in Fig. 3.

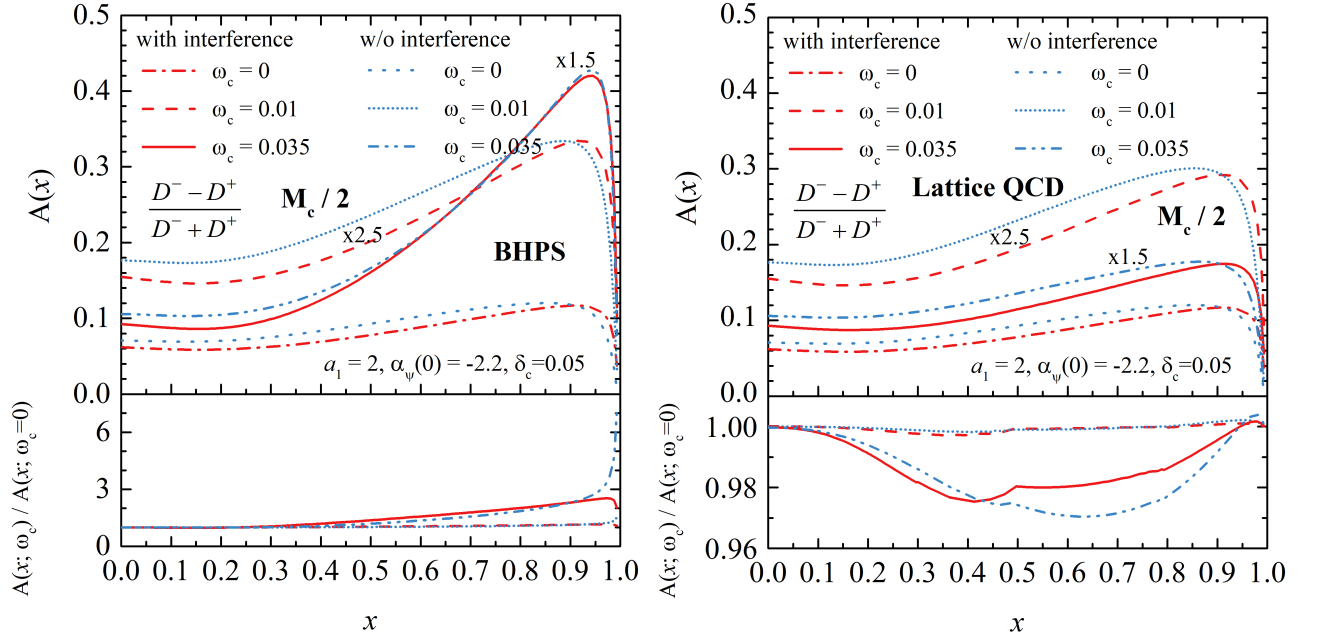


Figure 6: The plots of the asymmetry $A_{D^-D^+}(x)$ for the mass of intrinsic quark $M_Q = M_c/2$ with the same notations as in Fig. 3.

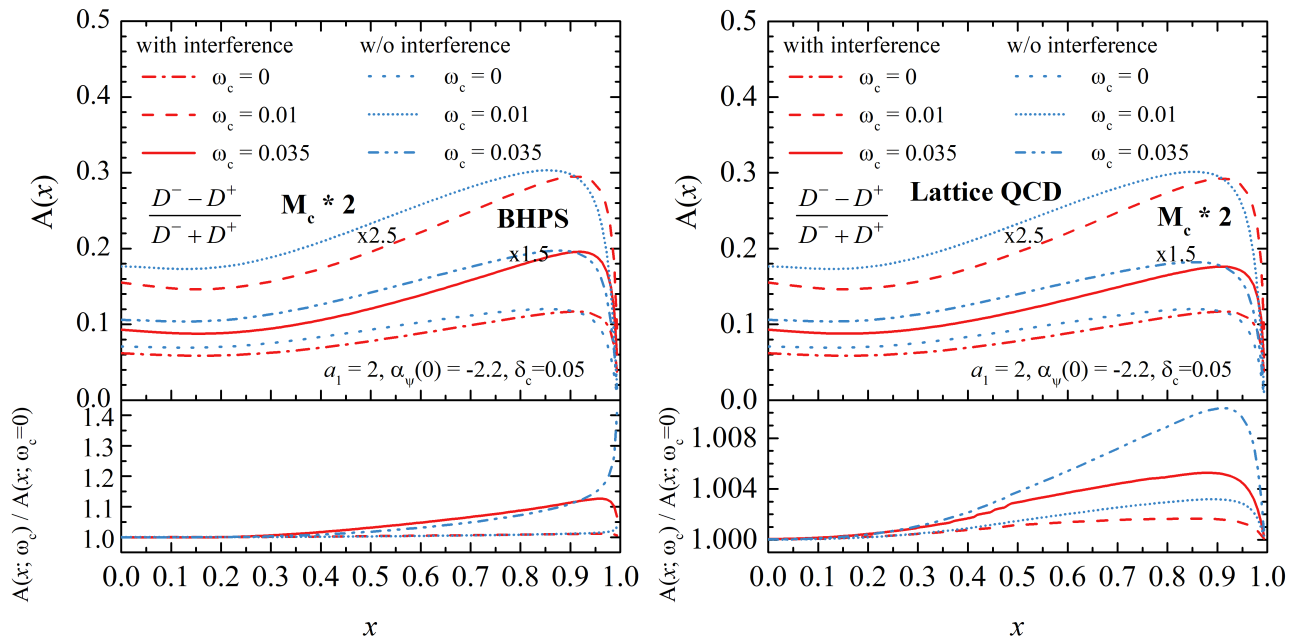


Figure 7: The plots of the asymmetry $A_{D^-D^+}(x)$ for the mass of intrinsic quark $M_Q = M_c * 2$ with the same notations as in Fig. 3.

paper [11].

The experimental data of WA82 [41] and E769 [42] for $D\bar{D}$ production in π^-p production at initial momenta 250 GeV/c and 340 GeV/c display an increase of the D^-D^+ asymmetry as a function of x , consistent with the calculation of $A_{D^-D^+}(x)$ presented in Fig. 4.

In Fig.(5) the asymmetries D^+D^- (left) and $D^0\bar{D}^0$ (right) are presented for the symmetric IC distribution given by Eq. (13). Comparing Fig.(4) and Fig.(5) one can see that both asymmetries change sign if the asymmetric IC distributions are included. This is a very important signal for identifying the IC contribution in the proton.

Let us study the sensitivities of D^+D^- asymmetry to the mass of intrinsic heavy quarks M_Q . In Figs.(6,7) the asymmetries as functions of x are presented at $M_Q = M_c/2$ and $M_Q = M_c * 2$. One can see from these figures that the *Set 1* calculation, taking into account the IC contribution, shows the increase of the asymmetry if M_Q decreases.

The string model (QGSM) we have used, as it mentioned in Section 2, is based on the $1/N$ topological expansion of the $h-h$ interaction amplitude proposed in refs. [21, 22] instead of an α_s expansion in perturbative QCD. This approach, developed later in ref. [23, 24] operates with the quark (valence and sea) and diquark distributions in the proton, and gluons are considered as $q\bar{q}$. Subprocesses of type the gluon splitting into $c\bar{c}$, which result in the *extrinsic* $c\bar{c}$ pairs, as calculated within perturbative QCD, are considered as the sea charm-anticharm pairs, taking into account their weight δ_c (Eq. 9) determined from a fit of experimental data for the open charm production. A central question is the contributions of *extrinsic* and *intrinsic* $c\bar{c}$ pairs and their interference to the D^-D^+ asymmetry. We have estimated it within the QGSM, and the results are presented in Fig. 4.

6. Conclusion

The D -meson production in pp collisions predicted by nonperturbative QCD, taking into account the intrinsic charm content in the proton has been analyzed. We have investigated

the relation of the $c\bar{c}$ non-perturbative intrinsic charm-anticharm asymmetry of the proton eigenstate as obtained from a QCD lattice gauge theory calculation of the proton's $G_E^p(Q^2)$ form factor [9] to the asymmetry $A_{D^-D^+}(x)$ and $A_{D^0\bar{D}^0}(x)$ of D -meson and \bar{D} -mesons produced in pp collisions at large x .

We have shown that the inclusion of the asymmetric IC components in the proton as calculated within the meson cloudy-bag model [37] leads to the enhancement of the D^-D^+ asymmetry at $x > 0.7$. The IC signal of this asymmetry depends on the intrinsic charm probability w_c . The maximal deviation of the D^-D^+ asymmetry compared to the prediction for zero IC is about 50% at $x \simeq 0.9$ and $w_{IC} = 3.5\%$. In principle, such a deviation in the range of 15%-20% can be experimentally observed.

As for the $D^0\bar{D}^0$ asymmetry in pp collisions, the IC signal is too small, less than 1% even at large IC probability $w_c = 3.5\%$.

In contrast, the x -spectra of $D\bar{D}$ and D^-D^+ -mesons calculated within the SM at large x are almost insensitive to the IC signal, because it is mostly determined by the diquark x -distributions at large x , which do not take into account the IC effect. The *extrinsic* and *intrinsic* sea quark distributions in the proton are also suppressed compared to the diquark distribution at large x . However, the IC signal can be visible at the asymmetry of D^-D^+ -mesons. As mentioned in Sect. 4, the large diquark contributions at large x are almost canceled in the difference $d\sigma_{D^-}/dx - d\sigma_{D^+}/dx$, see Eq.(25) for the D^-D^+ asymmetry. The IC contributions are not canceled due to their asymmetrical x -dependence. This leads to an enhancement of the D^-D^+ asymmetry at large x . It is shown that the $D^+ - D^-$ asymmetry increases if the intrinsic quark mass M_Q decreases, as it can be seen in the left bottom of Fig. 4. Therefore, the contribution of the strange-antistrange intrinsic quarks (IS) to the asymmetry of strange-antistrange hadrons could be larger than the IC one to the D^+D^- asymmetry. More detailed theoretical analysis of this effect can be done as the next step calculating IS distributions [14, 39] and taking into account different fragmentation functions of quarks to strange hadrons.

There is another interesting and very important result. The asymmetry of D^+D^- and $D^0\bar{D}^0$ mesons changes the sign by the inclusion of the asymmetric IC distribution instead of the symmetric one.

This paper thus confirms the important role of the $c\bar{c}$ asymmetry for the IC content in the proton as obtained from lattice gauge theory in ref. [9] and observations [11] of the $c\bar{c}$ asymmetry from $Z + c$ production in pp collisions at the LHC [15].

7. Acknowledgments

We are very grateful to R.S. Sufian for the data file of $\Delta c(x) = [c(x) - \bar{c}(x)]$ obtained within the lattice QCD which was essential for our calculations. We also thank V.A. Bednyakov for useful discussions. This work was supported in part by the Dept. of Energy Contract No. DE-AC02-76SF00515. SLAC-PUB-17763.

8. Appendix

8.1 Interference effects

In the standard QGSM, the interference between different topological graphs are not included. Let us try to take into account the interference terms between different parton contributions, including the contributions of extrinsic and intrinsic $c\bar{c}$ pairs to the inclusive spectrum of D -mesons $\rho_h(x)$ presented by Eq. 1. The relative phase between these

contributions is unknown, therefore we can estimate the maximum of this interference assuming the constructive sum squared of the all amplitudes in the inclusive x -spectrum. Thus, the inclusive x -spectrum of D -mesons:

$$\rho_D(x) = \int E \frac{d^3\sigma}{d^3p} d^2p_\perp = \sum_{n=0}^{\infty} \sigma_n(s) \varphi_n^D(s, x), \quad (26)$$

can be also presented in the form:

$$\rho_{Dtot} = \sum_{n=1}^{\infty} \sigma_n(s) \phi_n^D(s, x) = (\sqrt{A_1} + \sqrt{A_2})^2, \quad (27)$$

where

$$A_1 = a^D \sum_{n=1}^{\infty} \sigma_n \{ F_{qV}^{D(n)}(x_+) F_{qq}^{D(n)}(x_-) + F_{qq}^{D(n)}(x_+) F_{qV}^{D(n)}(x_-) \} \quad (28)$$

and

$$A_2 = a^D \sum_{n=1}^{\infty} \sigma_n 2(n-1) F_{q_{sea}}^{D(n)}(x_+) F_{\bar{q}_{sea}}^{D(n)}(x_-) \quad (29)$$

where A_2 has both extrinsic and intrinsic $c\bar{c}$ contributions. We have calculated A_2 at $\omega_c = 0.0, 0.01, 0.035$, and at different $c\bar{c}$ weights in the proton $\delta_c = 0.01$ and $\delta_c = 0.05$. The term A_1 does not have both extrinsic and intrinsic $c\bar{c}$ contributions.

8.2 Fragmentation functions for D^+ meson

Let us present the fragmentation functions of quarks, diquarks into D -mesons (FF) used within the QGSM [32].

Valence quark, diquark FF into D^+ meson:

$$G_d^{D^+}(x) = G_u^{D^+}(x) = (1-x)^{\lambda-\alpha_\psi(0)+2(1-\alpha_R)} \quad (30)$$

$$G_{uu}^{D^+}(x) = G_{ud}^{D^+}(x) = (1-x)^{\lambda-\alpha_\psi(0)+2(\alpha_R-\alpha_N)+1} \quad (31)$$

Sea quark FF into D^+ meson:

$$G_{\bar{u}}^{D^+}(x) = G_{\bar{d}}^{D^+}(x) = G_d^{D^+}(x) = (1-x)^{\lambda-\alpha_\psi(0)+2(1-\alpha_R)} \quad (32)$$

$$G_{\bar{d}}^{D^+}(x) = (1-x)^{\lambda-\alpha_\psi(0)}(1+a_1x^2) \quad (33)$$

$$G_c^{D^+}(x) = G_{\bar{c}}^{D^+}(x) = x^{1-\alpha_\psi(0)}(1-x)^{\lambda-\alpha_R} \quad (34)$$

8.3 Fragmentation functions for D^- meson

Valence quark, diquark FF into D^- meson:

$$G_u^{D^-}(x) = (1-x)^{\lambda-\alpha_\psi(0)+2(1-\alpha_R)} \quad (35)$$

$$G_d^{D^-}(x) = (1-x)^{\lambda-\alpha_\psi(0)}(1+a_1x^2) \quad (36)$$

$$G_{ud}^{D^-}(x) = (1-x)^{\alpha_R-2\alpha_N+\lambda+\Delta\alpha+1}(1+(a_1x^2)/2) \quad (37)$$

$$G_{uu}^{D^-}(x) = (1-x)^{\alpha_R-2\alpha_N+\lambda+\Delta\alpha+1} \quad (38)$$

Sea quark FF into D^- meson:

$$G_{\bar{u}}^{D^-}(x) = G_{\bar{d}}^{D^-}(x) = G_u^{D^-}(x) = (1-x)^{\lambda-\alpha_\psi(0)+2(1-\alpha_R)} \quad (39)$$

$$G_{\bar{d}}^{D^-}(x) = (1-x)^{\lambda-\alpha_\psi(0)}(1+a_1x^2) \quad (40)$$

$$G_c^{D^-}(x) = G_{\bar{c}}^{D^-}(x) = x^{1-\alpha_\psi(0)}(1-x)^{\lambda-\alpha_R} \quad (41)$$

8..4 Fragmentation functions for the D^0 meson

Valence quark, diquark FF into D^0 meson:

$$G_d^{D^0}(x) = G_u^{D^0}(x) = (1-x)^{\lambda-\alpha_\psi(0)+2(1-\alpha_R)} \quad (42)$$

$$G_{uu}^{D^0}(x) = G_{ud}^{D^0}(x) = (1-x)^{\lambda-\alpha_\psi(0)+2(\alpha_R-\alpha_N)+1}(1+a_1x^2) \quad (43)$$

Sea quark FF into D^0 meson:

$$G_{\bar{d}}^{D^0}(x) = G_d^{D^0}(x) = G_u^{D^0}(x) = (1-x)^{\lambda-\alpha_\psi(0)+2(1-\alpha_R)} \quad (44)$$

$$G_{\bar{u}}^{D^0}(x) = (1-x)^{\lambda-\alpha_\psi(0)}(1+a_1x^2) \quad (45)$$

$$G_c^{D^0}(x) = G_{\bar{c}}^{D^0}(x) = x^{1-\alpha_\psi(0)}(1-x)^{\lambda-\alpha_R} \quad (46)$$

8..5 Fragmentation functions for the \bar{D}^0 meson

Valence quark, diquark FF into \bar{D}^0 meson:

$$G_d^{\bar{D}^0}(x) = (1-x)^{\lambda-\alpha_\psi(0)+2(1-\alpha_R)} \quad (47)$$

$$G_u^{\bar{D}^0}(x) = (1-x)^{\lambda-\alpha_\psi(0)}(1+a_1x^2) \quad (48)$$

$$G_{ud}^{\bar{D}^0}(x) = (1-x)^{\alpha_R-2\alpha_N+\lambda+\Delta\alpha} \quad (49)$$

$$G_{uu}^{\bar{D}^0}(x) = (1-x)^{\alpha_R-2\alpha_N+\lambda+\Delta\alpha} \quad (50)$$

Sea quark FF into \bar{D}^0 meson:

$$G_{\bar{d}}^{\bar{D}^0}(x) = G_u^{\bar{D}^0}(x) = G_d^{\bar{D}^0}(x) = (1-x)^{\lambda-\alpha_\psi(0)+2(1-\alpha_R)} \quad (51)$$

$$G_u^{\bar{D}^0}(x) = (1-x)^{\lambda-\alpha_\psi(0)} \quad (52)$$

$$G_c^{\bar{D}^0}(x) = G_{\bar{c}}^{\bar{D}^0}(x) = x^{1-\alpha_\psi(0)}(1-x)^{\lambda-\alpha_R} \quad (53)$$

$\lambda = \alpha_R = 0.5$; $\alpha_N = -0.5$; $\alpha_\psi(0) = -2.2$ or $\alpha_\psi(0) = 0$; $a_1 = 2$ or $a_1 = 30$;
 $\Delta\alpha = \alpha_R - \alpha_\psi(0)$

References

- [1] S.J. Brodsky, P. Hoyer, C. Peterson, N. Sakai, Phys. Lett. B **93**, 451 (1980).
- [2] Stanley J. Brodsky, John C. Collins, Stephen D. Ellis, John F. Gunion, John F., Alfred H. Mueller, DOE/ER/40048-21 P4, SLAC-PUB-15471, (1984).
- [3] M. Franz, M.V. Polyakov, K. Goeke, Phys.Rev. D**62** 074024 (2000).
- [4] B.W. Harris, J. Smith, R. Vogt, Nucl.Phys. B**461**, 11 (1996).
- [5] S.J. Brodsky, A. Kusina, F. Lyonnet, I. Schienbein, H. Spiesberger, R. Vogt, Adv. High Energy Phys., **2015**, 23154 (2015).
- [6] F.S. Navarra, Marina and Nunes, M. Teixeira, Phys.Rev. D**54** 842 (1996).
- [7] J. Pumplin, Phys.Rev. D**73**, 114015 (2006).

- [8] S.J. Brodsky, K.Yu-Ju. Chiu, Jean-Philippe Lansberg, N. Yamanaka, Phys. Lett. **B783**, 287 (2018).
- [9] R.S. Sufian, T. Liu, A. Alexandru, S.J. Brodsky, G. F. de Téramond, H.G. Dosch, T. Draper, Keh-Fei Liu, Yi-Bo Yang, Phys. Lett. B **808**, 135633 (2020).
- [10] G. F. de Teramond and S. J. Brodsky, Phys. Rev. Lett. **94**, 201601 (2005) doi:10.1103/PhysRevLett.94.201601 [arXiv:hep-th/0501022 [hep-th]].
- [11] R.D. Ball, et al., arXiv:231100743 [hep-ph]
- [12] S.J. Brodsky, G.I. Lykasov, A.V. Lipatov, J. Smiesko, Prog.Part.Phys., **114**, 10302 (2020).
- [13] Collaboration, Nature **68**, 483 (2022), arXiv:2208.0832 [hep-ph].
- [14] V.A. Bednyakov, S. Brodsky, A.V. Lipatov, G.I. Lykasov, J. Smiesko, S. Tokar, Eur.Phys. J C **79**, 92 (2019); arXiv:171.209096 [hep-ph].
- [15] LHCb Collaboration, R. Aij, et al., Phys.Rev.Lett. **128**, 082001 (2022)
- [16] EIC M. Kelsley, et al., Phys.Rev. D **104**, 054002 (2021).
- [17] M.Guzzi, et al., Phys.Lett. B **843**, 137975 (2023), arXiv:2211.01387 [hep-ph].
- [18] A. Courtoy, et al., Phys.Rev. D **107**, 034008 (2023), arXiv:2205.10444 [hep-ph].
- [19] Tie-Jiun Hou, et al., JHEP, **2018**, 59 (2018), arXiv:1707.00657 [hep-ph].
- [20] L.A. Harland-Lang, T. Cridge, R.S. Thorne, arXiv:2407.07944 [hep-ph].
- [21] G. t'Hooft, Nucl.Phys., **B72**, 461 (1974).
- [22] G. Veneziano, Phys.Lett. **B52**, 220 (1974).
- [23] A.B. Kaidalov, Phys.Lett. **B116**, 459 (1982).
- [24] A. Capella U. Sukhatme, C.-I. Tan, J. Tran Thanh Van, Phys.Rep., **236**, 225 (1994).
- [25] A.B. Kaidalov, Z. Phys., **C12**, 63 (1982).
- [26] K.A. Ter-Martirosyan, Phys. Lett. B **44**, 377 (1973).
- [27] A.B. Kaidalov, O.I. Piskunova, Production of charmed particles in the quark-gluon string model. Sov. J. Nucl. Phys. **43**, 994 (1986)
- [28] A.B. Kaidalov, O.I. Piskunova Z. Phys. C **30**, 145 (1986)
- [29] S.I. Sinegovsky, M.N. Sorokovikov, Eur.Phys.J., C **80**, 4 (2020).
- [30] Yu.M. Shabelski, Sov. J. Nucl. Phys. **44**, 117 (1986)
- [31] LEBC-EHS Collab., M. Agilar-Benitez, et.al., Z.Phys. C **40**, 321 (1988).
- [32] G.I. Lykasov, G.G. Arakelyan, M.N. Sergeenko, The quark gluon string model: soft and semihard hadronic processes. Phys. Part. Nucl. **30**, 343 (1999)
- [33] G.H. Arakelyan, P.E. Volkovitsky, Charmed particle production in hadron-hadron collisions. Z. Phys. A **353**, 87 (1995).

- [34] S.J. Brodsky, C. Peterson, N.Sakai, Phys.Rev., D 23, 2745 (1981).
- [35] J. Bluemlein, Phys.Lett., B **753**, 619 (2016).
- [36] M.V. Pollyakov, A. Shafer,O.V. Teryaev, Phys.Rev., D 60, 051502 (1999).
- [37] J. Pumplin, H.L. Lai, W.K. Tung, Phys.Rev., D 75, 054029 (2007).
- [38] LEBC Collaboration. R.Ammar et al., Z.Phys. C **40** 321 (1981).
- [39] Jen-Chien Peng, Wen-Chen Chang, arXiv:1207.2193.
- [40] Yu.M. Shabelski, Surveys in High En.Phys., **9**, 1 (1995)
- [41] M. Adamovich, et al., Phys.Lett.,B **395**,402 (1993).
- [42] G.A. Alves, et al., Phys.Rev.Lett.B **72**, 812 (1994).